ORIGINAL ARTICLE

The Structural and Functional Connectivity of the Pineal Gland, and its Age and Gender Associations

Pejman Kiani [1,2], Gholamreza Hassanzadeh [3,4,5], Seyed Amir Hossein Batouli [3,6]*

[1] *Department of Radiology, School of Paramedical Sciences, Guilan University of Medical Sciences, Rasht, Iran*

[2] *Guilan Road Trauma Research Center, Trauma Institute, Guilan University of Medical Sciences, Rasht, Iran*

[3] *Department of Neuroscience and Addiction Studies, School of Advanced Technologies in Medicine, Tehran University of Medical Sciences, Tehran, Iran*

[4] *Department of Anatomy, School of Medicine, Tehran University of Medical Sciences, Tehran, Iran*

[5] *Department of Tele-Health, School of Medicine, Tehran University of Medical Sciences, Tehran, Iran*

[6] *BrainEE Research Group, Tehran University of Medical Sciences, Tehran, Iran*

*Corresponding Author: Seyyed Amir Hossein Batouli
Email: batouli@sina.tums.ac.ir

Received: 05 April 2024 / Accepted: 01 March 2025

Abstract

Purpose: The pineal gland (PG) is a structure located in the midline of the brain, and is considered the main part of the epithalamus. There are reports on the role of this area for brain function by hormone secretion, as well as few reports on its role in brain cognition. However, little knowledge is available on the structural and functional connectivity of the PG with other brain regions, as well as its age and gender associations.

Materials and Methods: In this work, we used the diffusion and resting-functional MRI data of 282 individuals, in the age range of 19 to 76 years old. All participants were checked for their medical and mental health by a general practitioner, and the MRI data were collected using a 3 Tesla scanner. The diffusion data were analyzed using the Explore DTI software (version 8.3), and the fMRI data were analyzed using the CONN toolbox (version 18.0).

Results: Two white matter tracts connecting the PG Body to PG Roots and PG to Pons were extracted in this study. The mean FA of the two tracts were 0.26 ± 0.06 and 0.24 ± 0.08, respectively. Neither the FA values of the tracts nor their lengths, showed any associations with age and gender; However, with increasing age, the likelihood of successfully identifying the PG-Pons tract decreased. In functional connectivity analysis, five brain regions showed positive connectivity with the PG, including the superior temporal gyrus, middle temporal gyrus, brain stem, vermis, and the subcallosal cortex, and 25 regions showed negative connectivity. These connectivities did not show an association with gender, but some associations with age were observed.

Conclusion: This study is novel in estimating the functional and structural connectivity of the PG with other brain areas, and also in assessing the association of these connections with age and gender, which could help to increase our knowledge on the functional neuroanatomy of the pineal gland.

Keywords: Pineal Gland; Diffusion Tensor Imaging; function Magnetic Resonance Imaging; Structural Connectivity; Functional Connectivity.

DOI:

1. Introduction

The Pineal Gland (PG) is located in the center of the brain in the roof of the third ventricle. It is between the two cerebral hemispheres [1]. The PG is part of the epithalamus and lies on the sagittal line of the brain. It is cone-shaped and reddish-grey in color, its length is 5 to 9 mm and its weight is 100 to 180 mg [2]. The pineal stem connects the PG to the diencephalon. The pineal peduncle is connected to the posterior commissure. The lower root of its peduncle makes this connection. It is also connected to the habenular commissure by the upper root of its peduncle [3]. Both the central nervous system and the peripheral ganglia innervate PG. Sympathetic and parasympathetic nerves innervate the PG. It also has central innervation. The sympathetic branch comes from the superior cervical ganglion. The parasympathetic branch comes from the sphenopalatine and optic ganglia. The central innervation branch comes from the brain. It enters the brain through the PG stem [4]. In humans, the growth of this organ is almost complete by the age of two. There are reports on changes in the weight and size of this organ after age two. There are also reports on a positive relationship between its size and melatonin levels [5].

As a photoneuroendocrine organ, the pineal gland plays a complex role in regulating circadian rhythms and hormone synthesis [1]. Light stimuli regulate the main hormone produced, melatonin [2, 6]. The main site of melatonin biosynthesis in vertebrates is the PG gland. The retinohypothalamus (RHT) projects to the brain's main pacemaker, the suprachiasmatic nucleus (SCN). Information from the SCN is then transmitted to the paraventricular nucleus (PVN) [7]. Its fibers descend to connect with the lateral and medial columns of the thoracic spinal cord (IML). The projections of the IML then ascend to the Superior Cervical Ganglion (SCG). Postganglionic SCG sympathetic fibers then ascend to the cells of the pineal gland. They go via the internal carotid canal. This happens in a nerve bifurcation called the "nervi conarii". They travel along with the internal carotid artery [5]. In addition to melatonin secretion, some studies found that the pineal gland is smaller in patients with Alzheimer's disease [8]. Other research suggests the pineal gland may also affect memory [9, 10]. In obese individuals, the pineal gland is also slightly smaller than normal [11]. In one study [12], researchers found that sexual maturation and growth of the reproductive organs were linked. Another study [13] found that PG size is smaller in sudden infant death syndrome. And, in another study [14], researchers found a positive link between PG size and Attention Deficit Hyperactivity Disorder (ADHD).

DTI is a non-invasive method for investigating the shape, density, and integrity of the myelin sheath of white matter [15]. It works by examining the diffusion of water molecules along the axon by applying a gradient [16]. Diffusion measurement by MRI is crucial for understanding biological tissues, as it allows for the assessment of water movement along specific axes. This heterogeneous diffusion reveals valuable anatomical information about living tissues. Key parameters such as fractional anisotropy (FA), Radial Diffusivity (RD), Mean Diffusivity (MD), and Axial Diffusivity (AD) provide insights into tissue structure. The alignment of fibers within white matter is particularly significant, as it reflects the underlying organization and integrity of neural pathways, enhancing our understanding of brain anatomy and function [17]. The structures within the white matter revealed by fiber orientation properties are important. One of the main applications of DTI is the ability to perform virtual dissections. It also describes microstructural changes in the living human brain [18]. Recent advances in diffusion imaging, such as increased signal-to-noise ratio and reduced scan time [19] enable imaging of thinner tracts and cross fibers. Tractography with constrained spherical deconvolution (CSD) [20] has also helped build this capability [21-23].

Resting-state functional MRI (rs-fMRI) is a cutting-edge technique for evaluating brain functional connectivity. It leverages hemodynamic responses linked to variations in oxyhemoglobin and deoxyhemoglobin concentrations, which alter the T2* relaxation time. By capturing spontaneous fluctuations in the Blood Oxygen Level-Dependent (BOLD) signal, rs-fMRI reveals the brain's intrinsic activity during rest. This method not only enhances our understanding of brain physiology but also elucidates the interconnectivity among various brain regions, providing a comprehensive view of the brain's functional architecture [24].

In our search of the literature, we did not find any studies that investigated the function or functional relationships of the pineal gland. The studies mainly aimed to investigate the pineal gland's function in producing melatonin. They also focused on studying melatonin's impact on the quality and quantity of nighttime sleep [25-27]. Concerning the structural connectivity of the PG, we did not find any research study on the subject. However, DTI has been used previously to study the subcortical white matter bundles. For example, the stria medullaris tracts were extracted [28]. The corpus callosum has also been examined using DTI in schizophrenia patients [29], and post-mortem studies show the brain stem realized the high sensitivity of the tractography method [30].

Despite the growing evidence of PG's role in several brain functionality, in our search of the literature, we found a scarcity of research on the pineal gland's functional and structural connectivities with the brain. In the context of its critical role in diverse neurological function and hormone production, the current study aims to investigate the functional and structural connections of the PG with other brain areas, and for this purpose, we hypothesized that:

1. The PG shows structural connectivity with the pons via the Nervi Conarii.

2. The PG shows functional connectivity with brain regions involved in circadian rhythm regulation, such as the SCN and hypothalamus.

3. These connections of PG may be correlated with age and gender.

Therefore, to address the current gap in knowledge, we used the structural, resting fMRI, and Diffusion-weighted MRI scans of 282 mentally and physically healthy individuals, in the age range of 19 to 76 years old. These data were collected using a 3T MRI scanner and a 64-channel head coil. We hope that our endeavor here could be a help to enhance our knowledge on the neuroanatomy of the pineal gland and the associated brain regions.

2. Materials and Methods

2.1. Participants

This study analyzed MRI data from 282 healthy individuals aged 19 to 77 years, sourced from the Iranian Brain Imaging Database (IBID). Initially, 301 MRI scans were collected; however, 18 scans were excluded due to quality issues. The participants had a mean age of 42.1 ± 13.5 years, with **67.6%** being under 50 years of age. The sample included 53.4% females, ensuring a balanced representation across genders. The age distribution is illustrated in Figure 1, highlighting the diverse age range represented in this dataset.

Based on IBID, Participants were selected based on the following inclusion and exclusion criteria:

2.2. Inclusion Criteria

- Healthy individuals with no significant medical or neurological conditions.

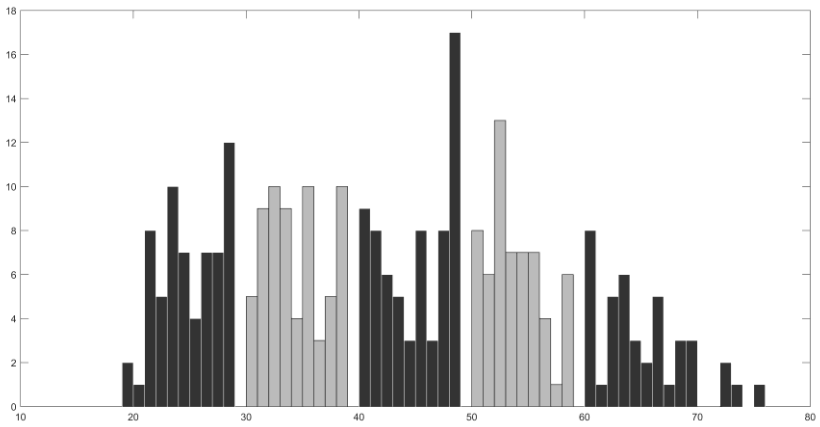

Figure 1. Age distribution of the participants in our study. They were aged between 19 and 76 years. The vertical axis shows the number of participants in each age group

- Weight less than 110 kg.
- No history of drug or alcohol addiction.
- No claustrophobia.
- Normal mental health, assessed using the Persian version of the Depression Anxiety Stress Scales (DASS-21) [31].

2.3. Exclusion Criteria

- Diagnosed medical or neurological conditions.
- Current or past medication use.
- History of chronic headaches, tinnitus, dizziness, seizures, or nausea.
- Family history of significant diseases.
- Surgical history involving anesthesia.
- History of loss of consciousness or head trauma.
- Presence of metal objects in the body (e.g., pacemakers, dental braces).

Each participant underwent a comprehensive clinical examination conducted by a general practitioner. This examination included assessments of blood pressure, heart rate, breathing rate, and a neurological evaluation encompassing vision and hearing [32].

2.4. Demographic Characteristics

The demographic profile of the sample is characterized by a diverse age distribution and gender representation, with participants recruited from various geographic regions in Iran. This broad representation reflects potential regional health disparities and cultural differences.

Although the age distribution is illustrated in Figure 1 and indicates a range between 19 to 77 years, we acknowledge that our sample may not fully represent the broader Iranian population. Factors such as socioeconomic status, educational background, and urban versus rural residence can significantly affect health profiles and brain imaging outcomes. The relative homogeneity regarding these socioeconomic factors within our sample may limit the external validity of our findings.

Additionally, cultural contexts specific to the Iranian population may influence brain structure and function differently compared to more heterogeneous populations. Hence, while our findings contribute to the understanding of the PG's role in brain function, they should be interpreted with caution regarding their applicability to diverse demographic groups.

To enhance the generalizability of future studies, it is crucial to include larger and more representative samples that encompass a broader range of demographic factors, including age, gender, ethnicity, and geographic location. By achieving increased representation, researchers can ensure that findings are more reliably applicable across different segments of the population, ultimately contributing to a deeper understanding of the relationships being studied in various demographic contexts.

2.5. Potential Confounding Factors

In our study, we recognize the importance of addressing potential confounding factors that could influence brain connectivity results. While we implemented stringent inclusion and exclusion criteria to minimize confounding variables, it is essential to consider additional influences that may not have been entirely controlled.

2.5.1. Medical Conditions and Medications

Participants were required to be healthy individuals with no significant medical or neurological conditions, and those with any history of medication use were excluded. This rigorous screening serves to ensure our sample is relatively homogenous. However, there may still be undiagnosed or atypical conditions that could impact brain connectivity.

2.5.2. Lifestyle Factors

While we aimed to control for significant external influences, factors such as sleep patterns, diet, physical activity, and overall lifestyle may still play a crucial role in brain health and connectivity. Although our study did not systematically collect detailed data on these lifestyle factors, we acknowledge their potential impact on the findings.

2.6. Imaging

The MRI data used in this study were obtained using a Siemens 3 Tesla Prisma MRI scanner (2016), which was allocated to research at the National Brain Mapping Laboratory (www.nbml.ir). The patient's position for imaging was supine, and a 64-channel head coil to image the brain of the participants was used. The image acquisition was initiated with a three-plane localizer according to the objectives of the study, followed by two protocols with the following parameters:

T1-weighted MP-RAGE. TA = 4:12 min; TR = 1800 ms; TE = 3.53 ms; TI = 1100 ms; flip angle = 7 degrees; voxel size = 1.0×1.0×1.0 mm; multi-slice mode = sequential; FOV read = 256 mm; #slices = 160; phase encoding direction = anterior >> posterior; matrix size =256×256×160; averages = 1.

Diffusion-weighted: Two series of diffusion images including diffusion images 1 with b-value_1 = 0 s/mm²; and diffusion images 2 with b-value_2 = 1000 s/mm²; diffusion directions = 64; TA= 11:05 min; TR = 9900 ms; TE = 90 ms; voxel size = 2.0×2.0×2.0 mm; FOV read =256mm; #slices= 65; distance factor = 0; phase encoding direction= anterior >> posterior; measurement = 1; delay in TR= 0 ms; matrix size = 128×128×65; multislice mode = interleaved.

Resting state fMRI parameters: TA = 6 minutes; TR = 2500 milliseconds; TE = 30 milliseconds; flip angle = 90 degrees; voxel size = 3.0 x 3.0 x 3.0 mm; number of slices = 40; matrix size = 64 × 64 × 40; distance factor = 0; phase encoding direction = anterior >> posterior; average = 1; delay in TR = 0 seconds; measurement = 144; multi-slice mode = interleaved.

2.7. Statistical Power Analysis Results

To verify the statistical power for our analyses, we conducted post-hoc power analyses using G*Power software (Version 3.1.9.7), incorporating a medium effect size of 0.25, an alpha level of α = 0.05, and a total sample size of 282 participants. The results indicated an achieved statistical power of 0.88 for between-group comparisons, suggesting an 88% chance of detecting a true effect, which exceeds the conventional threshold of 0.80, indicating that our sample size is sufficient for identifying medium to large effects. For regression analyses predicting connectivity based on demographic factors, the power was 0.85, confirming adequate capacity to examine these associations. Additionally, the power for detecting correlations between connectivity measures was calculated at 0.90, reflecting a strong ability to identify significant relationships. Overall, these findings confirm that our study is well-powered to detect significant effects across all planned analyses, thereby enhancing the reliability and robustness of our conclusions.

2.8. Data Analysis

2.8.1. DTI Data Analysis

In this study, Explore DTI software (version 8.3) was used for data analysis. The dcm2nii toolbox facilitated the conversion of raw diffusion data into NIFTI and ExploreDTI formats. We generated a B matrix using. b_{val} and .b_{vec} files. We sorted the DWI images according to their b-values. We used the 'Convert raw data to DTI .mat' tool with optimal settings on all data. This included spatial dimension, spatial orientation, gradient components, number of non-DWI images, number of DWI images, and matrix size. The goal was to create the DTI .mat file. After obtaining the above results with high accuracy, we checked the quality of all the data. We did this both visually and using the software. Various artifacts (such as Gibbs ring and patient motion, eddy current, and distortion) were the target of identification. To address this, we corrected for subject motion and EC/EPI distortion in all data. The method used was the Robust Extraction of Kurtosis Indices with Linear Estimation (REKINDLE). It had a kappa value of 6. We then loaded the trafo.mat file and T1-weighted scans. Again the data quality was checked visually and by software. We checked the pre-processings for correctness and consulted with an expert familiar with the whole brain tractography procedure. We then checked the pre-processing with different parameters.

In our tractography study, we utilized Regions of Interest (ROIs) and logical conjunctions (ANDs) with DTI Explorer software. Initially, we identified the anatomical locations for the ROIs, ensuring precise placement based on anatomical knowledge. We drew at least two ROIs perpendicular to the anticipated tracts. This allowed us to determine the tracts associated with the pineal body and roots. The above

process was carried out to draw the tracts of the norepinephrine pathway from the nuclei of the supracervical ganglia (SCG) towards the pineal gland. Subsequently, we extracted key parameters, including fractional anisotropy (FA), tract length, and a number of tracs, documenting all results systematically.

2.8.2. Functional Connectivity Analysis

We preprocessed the resting-state fMRI data using CONN software, which is a Matlab-based toolbox. It calculates, displays, and analyzes functional connectivity in fMRI. This software uses connectivity metrics. These include seed-to-voxel connectivity maps, ROI-to-ROI connectivity matrices, graphical features of connectivity networks, and generalized psychophysiological interaction models (gPPI).

To perform connectivity analysis using this toolbox, we used both functional MRI data and anatomical or structural data. Functional data can be used in either resting or task mode. Structural data should include at least anatomical T1 images, used primarily for delineation. The CONN toolbox also provides a set of predefined ROIs. These ROIs are automatically loaded. For example, the ROIs include a segmentation of 91 cortical and 15 subcortical regions in the whole brain. They come from the Harvard FSL atlas. This software allows for importing specific ROIs. Due to the lack of a pineal ROI, we imported this ROI from the previous studies by Batouli and colleagues [17] into the software. To pre-process the data, we first loaded the functional and anatomical data into the CONN-tools software. Then, we pre-processed it using a flexible method. This method included realignment with magnetic receptivity correction, slice timing correction, outlier detection, direct segmentation, and normalization in the MNI space. We also performed smoothing. We used field-map images to calculate the phase difference. This helped remove image distortion in anatomical areas with high magnetic susceptibility (bone-air). Then, a map was created to remove the displacement of pixels. Not all slices were collected at the same time. There is a slight time difference. To correct for this, one slice was chosen as a reference. The remaining slices were then interpolated to match the reference slice. This was done for all the slices in the same order as for the first slice. This causes all the slices to overlap. A rigid registration step with six degrees of freedom (three degrees of coordinates and three degrees of rotation) was then performed to find and remove the movement artifacts of the patient. Next, we performed co-registration using T1 structural images. This helped us locate the functional activity in the anatomical area. Then, we performed image segmentation for white matter, grey matter, and CSF. We transformed the images into a standard space. We did this to report the functional areas of the brain that correspond to anatomical areas. This step also allows reliable averaging across different individuals and samples. We performed the normalization of the images in the so-called MNI space. This step is necessary for the analysis of group data. There is a lot of noise in the fMRI images, and therefore, these data were denoised by smoothing before statistical analysis. The frequency of noise is known to be high. So, data smoothing was done by data convolution with a Gaussian kernel. For this purpose, a Gaussian kernel of at least twice the size of the voxel (FWHM 8 mm) was applied. In this step, the signal intensity of each voxel was replaced by the average intensity of the neighboring signals. As expected, the images became somewhat blurred after smoothing. The above steps were also performed for structural images.

This study did not consider only one area, and we examined PG's connections with all brain areas that have the same functions. More precisely, it can be seen as the temporal correlation between the neurophysiological activities of the PG and other brain regions. These activities occur far from each other. Resting-state functional connectivity follows temporal correlation in the BOLD signal. In this study, we used rest functional connectivity that was preprocessed. After analyzing the activated regions in the brain, we performed a functional connectivity analysis on the rest-fMRI data of the observed brain regions. Therefore, we used the CONN v.18b toolbox for ROI-to-ROI connectivity. The toolbox is available at https://www.nitrc.org/projects/conn. Then, a seed-based fMRI connection was performed. ROIs were drawn along the PG pathway in the samples. We used the CONN toolbox to calculate functional connectivity. We used a high-pass filter of 0.008-0.09 Hz. Six movement-corrected parameters were included in the GLM model. Pearson's correlation was calculated in the whole brain. The difference between the groups was determined by the F test using a General Linear Model (GLM). The model assumed P-

FDR<0.05. These steps produced maps. The maps showed the possible functional connections between the PG and other brain regions. The maps also show the extent and pattern of these connections. These connections can have a positive or negative sign. They show if this area is functionally connected with other brain areas.

2.9. Statistical Analysis

Our statistical analysis for structural connectivity was performed using SPSS software (version 26) and CONN software for functional connectivity analysis. We set the threshold for statistical significance at p-FDR < 0.05, indicating that only results meeting this criterion were considered statistically significant. A range of statistical tests was employed to analyze the relationship between white matter (WM) indices—specifically fractional anisotropy, tract length, and tract number—and demographic variables such as age and sex.

To explore these correlations, we utilized both parametric and non-parametric tests. Analysis of Variance (ANOVA) and independent t-tests were applied to compare means of normally distributed data across multiple groups (e.g., age and sex). For data that did not meet the assumptions of parametric tests or when comparing non-normal data between groups, we employed Mann-Whitney U tests and Kruskal-Wallis tests**.**

To ensure that our statistical tests were valid, **we** conducted Shapiro-Wilk and Kolmogorov-Smirnov tests to verify that the data followed a normal distribution, a fundamental requirement for parametric analyses. Although not explicitly mentioned, we implicitly checked for equal variances between groups, which is essential for ANOVA and independent t-tests. By using non-parametric tests where necessary, we addressed cases where the assumptions for parametric tests might not have been satisfied. Additionally, we monitored multicollinearity via Variance Inflation Factor (VIF) calculations, ensuring that VIF values remained below the threshold of 10.

Addressing multiple comparisons is critical in our analyses, as failing to manage this aspect can lead to an increased risk of false positives. To ensure the integrity of our findings, we employed the false discovery rate (FDR) method for corrections. FDR is particularly suitable for our study, as it balances the identification of significant results while controlling the proportion of false discoveries among the declared significant findings. By applying the FDR correction, we adjusted our significance threshold (p-FDR < 0.05), ensuring that only results that genuinely reflect statistical significance are reported. This approach effectively mitigates the risk of Type I errors, thereby enhancing the robustness and validity of our conclusions.

2.10. WM Tracts Connected to the PG

The aim of this study was to determine the structural and functional relationships of the pineal gland with other brain areas. Therefore, to investigate the possibility of nerve tracts, based on the hypothesis that nerve tracts originating from the pineal gland pass through its roots, and that tracts from the superior cervical ganglia converge within the pineal gland, the Nervi Conarii tract was thoroughly examined. As DWI images of the patients had been acquired from the foramen magnum to the vertex, it was not possible to examine the path by drawing 3 ROIs

simultaneously, so in this study we examined the path of the Nervi Conarii to investigate the possibility of structural connections in two stages and by drawing separate ROIs. The path from the pineal gland to the supracervical ganglion (SCG), which in our study was called the PG-Body-Pons pathway. And the path of the tracts that left the PG and passed through the roots, which in our study was called the Pine Body-Pine Roots pathway.

3. Results

3.1. WM tracts connected to the PG

The aim of this study was to determine the structural and functional relationships of the pineal gland with other brain areas. Therefore, to investigate the possibility of nerve tracts, the Nervi Conarii tract was examined for this purpose, assuming that the tracts separated from the pineal gland must originate from the roots of the pineal gland and that the tracts of the super cervical ganglia would also enter the pineal gland. As the DTI information from the patients was

from the foramen magnum to the vertex, it was not possible to examine the path by drawing 3 ROIs simultaneously, so in this study we examined the path of the Nervi Conarii to investigate the possibility of structural connections in two stages and by drawing separate ROIs. The path from the pineal gland to the supracervical ganglion (SCG), which in our study was called the PG-Body-Pons pathway. And the path of the tracts that left the PG and passed through the roots, which in our study was called the Pine Body-Pine Roots pathway.

3.1.1. PG Body- PG Roots

Assume that the tracts originating from the pineal gland exit from the pineal roots. We used two ROIs to draw this possible tract. To draw the first ROI in the region of the pineal body, we determined the widest part of the pineal body in the axial view. Then, using the CROSS HAIRS tool of the EXPLORERDTI software, we determined the same cross-sectional area in both sagittal and coronal views. After selecting the appropriate slice at the indicated location, we drew an ROI around the pineal gland in the coronal view to include only the pineal gland. To draw the second ROI, after locating the pineal roots in the axial view using the CROSS HAIRS tool, the second ROI was drawn in the coronal view. Finally, an average number of 7 tracts was observed in the above route with an average FA = 0.252891 and the average length of the tracts was 79.74883. It was also observed that the supplementary motor area received branches from the PG in several cases (Figure 1).

3.1.2. PG Body-Pons

We used two ROIs to map the norepinephrine pathways that project from the supracervical nucleus (SCG) to the pineal gland. The first ROI was placed in the pineal body. To find the pineal body, we first scrolled through the T1 images in axial view and selected a section of the axial images where the largest diameter of the pineal could be seen. Then, by activating CROSS HAIRS in the EXPLORERDTI software, we were able to accurately determine the position of the pineal gland in the sagittal and coronal views. After determining the exact position of the pineal gland in the three views, the ROI was drawn in the body of the pineal gland in the coronal view. To draw the second ROI, assuming that the goal was to draw the norepinephrine tracts that come from the SCG to the gland, we drew the location of the ROI according to the aforementioned cases at the junction of the medulla with the pons in the coronal view, and the size of the ROI was chosen to include the entire cerebellum and the carotid arteries. In most cases where the tract was observed, the desired tract could be identified individually. In a number of patients, there was also a downward tract towards the cerebellum. However, it was so short that in all cases it could not be drawn according to the area we considered for drawing the ROI. Therefore, it was only visible in the cases where this tract was anatomically longer. This tract has an average FA =0.242 with an average length of 319.78 mm, which was identified in 68.85% of the cases (Figure 2 and Figure 3).

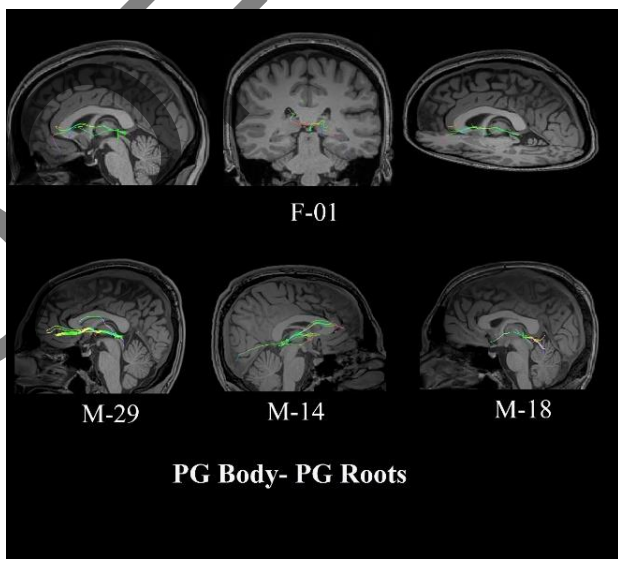

Figure 2. Structural MRI scans illustrating white matter tracts associated with the PG Body - PG Roots. The top row features images from patient F-01 with multiple views, while the bottom row presents images of various patients (M-29, M-14, M-18) in different planes. Tracts are color-coded for clarity

3.2. The statistical Analysis of the WM Tracts

According to the results of this study, the PG Body - PG Roots and the PG Body - PG Pons were observed in 96.4% and 56.5% of the samples, respectively.

The average FA of the PG Body-PG Roots tract in the research samples is 0.26 ± 0.06, the lowest value is 0.03 and the highest value is 0.43. The average tract length (in millimeters) in the samples is 76.82 ± 16.06, the lowest value is 26.40 and the highest value is 130.20. The results showed that there was no

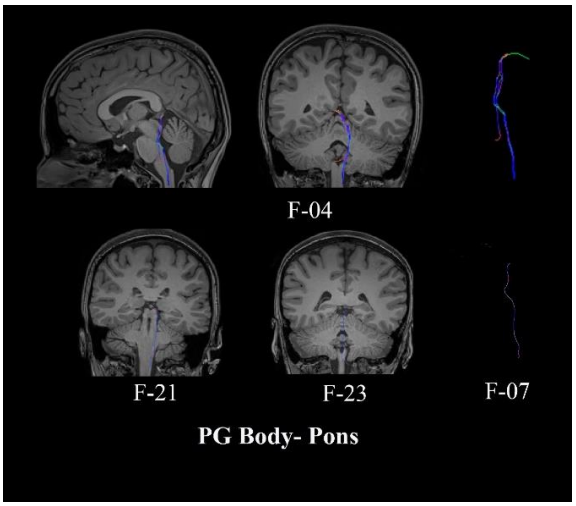

Figure 3. Structural MRI scans illustrating white matter tracts associated with the PG Body - Pons regions. The top row features images from patient F-04 with multiple views, while the bottom row presents images of various patients (F-21, F-23, F-07) in different planes. Tracts are color-coded for clarity

statistically significant relationship between the presence of PG Body-PG Roots tract with age and sex.

There was also no statistically significant relationship between FA and age and sex, nor between tract length and age and sex. With increasing age, the FA value increases slightly and the length value decreases slightly, but these changes are not statistically significant. As the FA value increases, the length value increases significantly. There was a statistically significant relationship between the number of tracts and age. With increasing age, the number of tracts increased. However, the relationship between the number of tracts and gender was not significant, although the number of tracts was higher in men than in women.

The results of this study on the PG-Pons tract showed that the average FA in the research samples was 0.24 ± 0.08, the lowest value was 0.09 and the highest value was 0.54. The average tract length in the samples was 73.96 ± 24.67, the lowest value was 49.00 and the highest value was 201.50.

There was a statistically significant relationship between the presence of the PG-Pons tract and age (P-value=0.005). It seems that the presence of the tract decreases with age. However, there was no significant relationship between this variable and sex (P-value=0.88). There is no statistically significant relationship between FA and age and gender, nor between tract length and age and gender. With increasing age, FA slightly increases and length slightly decreases, but these changes are not statistically significant. As the FA value increases, the length value increases significantly. There was no statistically significant relationship between the number of tracts and age and sex. In fact, with increasing age, the number of tracts increases slightly, but these changes are not statistically significant (Table 1 and Table 2).

3.3. The Functional Connectivity of the PG

The primary objective of this functional connectivity analysis is to investigate the neural networks and connections between the pineal gland and other brain regions in the resting state while accounting for individual differences in age and sex. To extract the functional connectivity of the pineal gland, we analyzed the functional connectivity in the resting state, taking into account age and sex, by calculating the ROI-to-ROI functional connectivity

Table 1. FA and tract lengths related to the pineal gland, including PG Body-PG Roots, are shown by age and gender, along with their relationships to these factors

FA (PG Body-PG Roots)				
P-Value	standard deviation	average		
0.670	.068	0.255	under 30	Age
	.062	0.261	30-40	
	.069	0.260	40-50	
	.055	0.273	50-60	
	.058	0.265	Above and equal to 60	
0.719	.059	0.264	Female	Sex
	.067	0.261	Male	
LENGTH (PG Body-PG Roots)				
	standard deviation	average		
	18.76	80.570	under 30	Age
	16.24	73.357	30-40	
	15.32	77.110	40-50	
	14.35	76.634	50-60	
	14.00	76.542	Above and equal to 60	
	16.15	76.709	Female	Sex
	16.00	76.948	Male	

Table 2. FA and tract lengths related to the pineal gland, including PG Body-Pons, are shown by age and gender, along with their relationships to these factors

FA (PG Body-Pons)				
P-Value	standard deviation	average		
	.07720	.2422	under 30	
	.0830	.2413	30-40	
	.0603	.2305	40-50	
0.489	.0724	.2379	50-60	Age
	.1127	.2888	Above and equal to 60	
0.205	.0839	.2380	Female	Sex
	.0782	.2534	Male	
LENGTH (PG Body-Pons)				
P-Value	standard deviation	average		
	27.7427	78.3192	under 30	
	12.9377	67.3449	30-40	
	18.2880	73.6213	40-50	
0.238	12.5650	67.7752	50-60	Age
	43.5000	85.6657	Above and equal to 60	
0.231	21.9521	71.9088	Female	Sex
	27.4486	76.3365	Male	

between the pineal gland and the brain regions to calculate the cross-correlation of brain areas. Statistically significant correlations between ROI pairs were determined using a general linear model (GLM) and assuming P-FDR <0.05. Positive correlations were shown in red and anti-correlations were shown in blue, as illustrated in Figure 4. Noise in fMRI data includes physiological, thermal, and motion-related sources. To control these, we used high-pass filtering and motion correction algorithms. We also applied a small smoothing kernel and accounted for nuisance variables in our analyses.

In this study, ROI to ROI functional connectivity was performed for all groups simultaneously according to the mentioned criteria, and the results were as follows. In the analysis of all data, as provided in Table 3, there was a positive correlation between the PG activity and the Vermis, Superior Temporal Gyrus, Subcallosal Cortex, Middle Temporal Gyrus, and brain stem. Also, negative functional connectivity was observed between the PG function and R Middle Frontal Gyrus, B Frontal Pole, L Fusifom, R

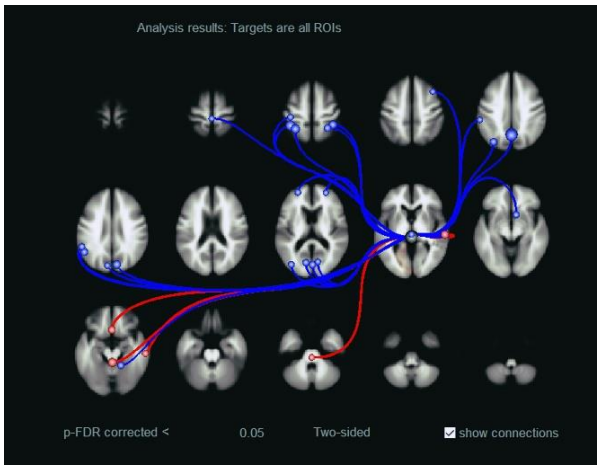

Figure 4. The pattern of the functional connectivity of the pineal gland with other brain regions is provided. A Red connectivity is positive, and a blue is negative. All connectivity measures are estimated based on a corrected p-value< 0.05 (FDR corrected)

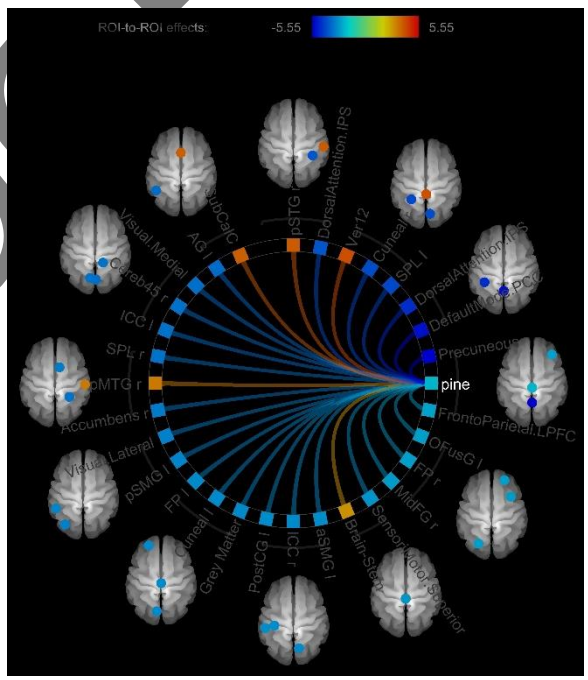

Figure 5. The thresholded ROI to ROI functional connectivity of the pineal gland with other brain regions; with positive (red) and negative (blue) functional connectivity in the PG. The brain regions are also illustrated on the diagram

Frontoparietal cortex, B cuneus, L postcentral G, B intracalcarine cortex, L supramarginal cortex, L supramargical cortex, R accumbens area, R cerebellum, B superior parietal G, L angular gyrus, lateral occipital cortex, posterior cingulate cortex, and precuneus. Details of these associations are better illustrated in Figure 5. In this analysis, to show the significance of the reported associations, we used the

P-FDR< 0.05, to control for dispersion and false discovery rate, and non-zero betas as a measure of the existence of connectivity.

This study also examined the association of functional connectivity with age and gender. There was no correlation with gender, but a significant and negative functional connectivity was observed between the PG and R superior temporal and subcallosal cortex. Our observation of a significant and negative correlation between the pineal gland (PG) and the right superior temporal and subcallosal cortex is a novel finding that warrants further examination. We propose that this association may be related to the pineal gland's role in regulating circadian rhythms and the superior temporal cortex's involvement in higher-order cognitive processes, such as attention and memory.

One possible explanation for this negative correlation is that the pineal gland's activity, which is influenced by the body's natural circadian rhythm, may modulate the activity of the superior temporal cortex in a way that is inversely proportional. In other words, as the pineal gland's activity increases, the activity of the superior temporal cortex may decrease, and vice versa. This could be because the pineal gland's melatonin secretion, which is highest at night and lowest during the day, may inhibit the activity of the superior temporal cortex, which is involved in attention and arousal.

Furthermore, the subcallosal cortex, which is a region involved in default mode processing and mind-wandering, showed a similar negative correlation with the pineal gland. This could suggest that the pineal gland's activity may also influence the brain's default mode network, which is involved in introspection and self-referential processing.

The finding that this correlation decreases with increasing age is also noteworthy. The observed decrease in functional connectivity with advancing age can be attributed to several potential mechanisms. One key factor is the natural decline in pineal gland function that occurs with aging. The pineal gland's primary role is to regulate circadian rhythms by secreting melatonin, which peaks at night and declines during the day. As people age, the pineal gland's ability to produce melatonin decreases, leading to disrupted circadian rhythms.

This disruption may, in turn, affect the brain's ability to regulate cognitive processes, such as attention and memory, which are modulated by the superior temporal cortex. As the pineal gland's activity decreases, the inhibitory effect on the superior temporal cortex may weaken, leading to altered cognitive processing.

Furthermore, age-related changes in the brain's neural circuits, such as reduced synaptic density and decreased neural plasticity, may also contribute to the decline in functional connectivity. These changes can impair the brain's ability to adapt to changing environmental demands and modulate cognitive processes.

The negative correlation between the pineal gland and the right superior temporal and subcallosal cortex may suggest a modulatory relationship between these regions. As the pineal gland's activity increases or decreases, it may have an inverse effect on the activity of these regions, potentially influencing cognitive processes like attention, memory, and default mode processing.

These findings have important implications for our understanding of the neural mechanisms underlying cognitive function and the potential contribution of the pineal gland to these processes. Further studies are needed to fully elucidate the mechanisms underlying this correlation and to explore its relevance to cognitive function in both healthy individuals and those with neurological or psychiatric disorders.

4. Discussion

In summary, we studied the functional and structural connectivity of the pineal gland. We focused on the nerve tracts of the Nervi Conarii for this purpose and verified that the tracts pass through the pineal roots. We identified the path between the SCG and the pineal gland, by examining the PG nerve path to the pons. We also evaluated the functional connections of the PG with other areas of the brain and observed positive and negative functional connectivity in this section. To the best of our knowledge, this is the first study to investigate the functional and structural connectivity of the pineal gland with all other brain regions.

4.1. Structural Connectivity of Pineal Gland

DTI is used extensively for tractography, by mapping the tracts identified by neuroanatomical knowledge or post-mortem studies [33-36], whereas initially these studies were performed without knowledge of neuroanatomy [33, 34, 37]. DTI studies have shown that the presylvian areas in the left hemisphere are connected by two parallel pathways. The pathways are direct and indirect neural pathways, although anatomical studies had previously confirmed the direct pathway. In this study, two ROIs were used to better distinguish the arcuate fasciculus. They confirmed this connectivity pattern and distinguished it from artifacts. They pointed to its repeatability in most of the samples studied. They also showed that the tracts can be found in most of the samples as a sign of the existence of variations [34]. Other studies have used DTI to identify neural tracts in areas of the human brain that cannot be examined directly. For example, the corticobulbar tract in the corona radiate [37]. This study has mapped the nervi conarii tract or pineal intervention. It is based on neuroanatomy knowledge. In summary, we studied the functional and structural connectivity of the pineal gland. We focused on the nerve tracts of the Nervi Conarii for this purpose and verified that the tracts pass through the pineal roots. We identified the path between the SCG and the pineal gland, by examining the PG nerve path to the pons. In our study, as in previous studies, two or more ROIs were used for tractography. This process shows fibers directly connecting areas of interest [33, 34]. In a study by S. Farquharson *et al.*, two tractography methods were compared: DTI-based and constrained spherical deconvolution (CSD). The CSD method, which does not require prior knowledge of fiber orientation in each voxel, effectively estimates fiber directionality. When applied to the corticospinal tract, the DTI method failed to accurately identify the tracts, while the CSD method successfully mapped all corticospinal tracts. This research highlights the significance of CSD in accurately assessing white matter pathways, particularly in contexts where fiber orientation is uncertain, such as with pineal tracts.[38]. The nervi conarii pathway is important. The SCN nuclei are the main pacemaker of melatonin secretion. A study showed the importance of this nucleus in circadian regulation. The study caused damage to the SCN nuclei of rats [39]. Kristin Koller and her colleagues reported that the nucleus is important for regulating circadian rhythm. They also reported on the neural pathway that causes circadian rhythm regulation [40]. These studies are fully consistent with our results, according to the PG-Pons pathway of our study. In their study, Møller M and colleagues reported that the PG is innervated by both sympathetic and parasympathetic nerves. The sympathetic nerves originate from the SCG. The parasympathetic nerves originate from the optic gangli [4]. The structural findings of our study show that these innervation pathways match the PG-Pons pathway for sympathetic nerves. The parasympathetic pathway in our study also matches the PG Head-PG Roots tract. In vivo dissection using DTI tractography has shown that the suprachiasmatic nucleus is the main circadian pacemaker. It regulates melatonin secretion through sympathopetal hypothalamic projections to the supracervical ganglia nuclei [40]. This is consistent with the results of our study. Clinically, these structural findings may have implications for understanding conditions involving disruptions in circadian rhythm, sleep disorders, and even mood disorders, given the PG's role in melatonin production. For example, disruptions in the PG-Pons pathway could potentially contribute to sleep disturbances observed in various neurological conditions.

4.2. Functional Connectivity of Pineal Gland

To investigate the functional connectivity of different brain regions, we used statistical analysis. This helps us identify these connectivities. To avoid false correlations, we must pay attention to noise sources. This is especially important when using GLM for this purpose. Therefore, because of the concepts in Mathematics and the possibility of noise, that may cause a shift in the distribution of correlation, we should be cautious in interpreting anticorrelations [41]. For this reason, the fMRI data were denoised by smoothing before statistical analysis.

Activation of the pineal gland is observed in some cognitive functions. For example, meditation can cause PG body activation [42]. It increases resting-state functional connectivity in different parts of the brain. This includes the posterior cingulate cortex and right middle temporal region [43]. We also evaluated the functional connections of the PG with other areas of the brain and observed positive and negative

functional connectivity in this section Meditation has been shown to engage the DMN, a network of brain regions, including the posterior cingulate cortex (PCC), medial prefrontal cortex (mPFC), and temporal lobes. The PCC, in particular, is a key node in the DMN. The study's finding of increased functional connectivity in the PCC suggests that meditation-induced activation of the pineal gland is associated with increased connectivity within the DMN. This network is involved in introspection, self-reflection, and mind-wandering, which are all characteristic of meditative states. Meditation has been shown to enhance the integration of sensory and cognitive information across different brain regions. The pineal gland's activation and the resulting increase in functional connectivity between regions may facilitate this integration, allowing for a more cohesive and unified perception of the self and the environment. The pineal gland's activation may also influence thalamocortical and corticocortical interactions, which are critical for sensory processing, attention, and cognitive functions. Meditation-induced changes in these interactions may contribute to the reported increases in functional connectivity between brain regions. The alignment of meditation-induced activation of the pineal gland with observed connectivity patterns suggests that this activation may play a key role in the cognitive and neural changes that occur during meditation. This aligns with our study's results. The decrease in sleep quality increases the functional connectivity between the hypothalamus and the vermis. As a result, sleepiness during the day also increases [44]. Patients with spinal ataxia or extensive cerebellar degeneration often experience daytime sleepiness. This happens because the cerebellum regulates the circadian rhythm [45]. This is completely consistent with our study. Functional connectivity between PG and vermis is present. Studies have been carried out to investigate the connectivity of the brainstem with other brain regions. One study used 7 Tesla MRI and precise noise methods to investigate the connectivity of brainstem nuclei. However, the study did not report the functional connections of this region with PG. This is inconsistent with our study [46]. Our study's findings regarding brainstem connectivity with the pineal gland (PG) differ from a previous study that used 7 Tesla MRI and precise noise methods. While the previous study investigated the connectivity of brainstem, it did not report the functional connections with the PG.

Because the previous study used the MNI atlas to select the target seed, which does not include a definition for the PG. In contrast, our study used a more precise PG atlas, allowing us to examine the connections in this area more accurately. Another hand the previous study aimed to investigate brainstem connectivity with other brain regions, whereas our study focused specifically on the PG and its connections with the brainstem.

These discrepancies highlight the importance of using precise and accurate anatomical definitions, such as the PG atlas, when examining the connections of specific brain regions. Our findings demonstrate the need for further research to investigate the neural mechanisms underlying the relationships between the brainstem, PG, and other brain regions. In one study, they showed that circadian regulation is associated with functional connectivity between the brainstem and ventrolateral preoptic nucleus. It has been suggested that due to the diversity of circadian phenotypes, there may be other regions involved in functional connectivity in the default mode network that should be investigated in studies [47]. The question here is whether it is possible to match or compare structural and functional results. Koch *et al.* compared the functional and structural connectivity of the cortical gyrus. They reported a positive relationship between them in the central sulcus [48]. The default mode network (DMN) in functional studies is inactive during tasks. It is active at rest [49, 50]. They found that studying this network showed functional connectivity does not always imply structural connectivity. Two areas may be functionally connected but lack a direct structural connection. A third party may help [51].

The regions identified in our study may have a functional relationship with PG. This may be due to their diverse circadian phenotype. It is also possible that the diversity of the regions involved in it contributes. A part was directly confirmed. It was assumed that the parts where there is no direct connection between structural and functional connections could be indirectly connected. In our study, we confirmed a functional connection between the pons and the brain stem. We did this by drawing the path of the pons. We confirmed the functional

connection of PG with the vermis in our structural study. We observed a tract from PG to the cerebellum in some data in the PG-Pons tract path. This tract is short. The location of the ROI was much lower than at the end of this tract, so it was not seen in all the data. The subcallosal cortex is part of the limbic system. It plays a role in controlling mood and feelings of sadness. On the other hand, the circadian rhythm is one of the main components of depression and the mode is known [11]. So, the subcallosal cortex may have an indirect functional relationship with PG. More studies are needed to confirm this possibility. The left superior temporal gyrus plays a role in speech and its temporal order. The right superior temporal gyrus plays a role in speech rhythm. Changing circadian and circadian sleep rhythms might regulate speech rhythm. It seems to do this by modulating the right superior temporal gyrus's PG. Alternatively, the hypothesis is that the multi-synaptic path of PG controls or modulates activity in different parts of the brain. This study found a significant correlation between the PG gland connections and age. This could be due to the gland's development until age two. Perhaps a study for children under two could observe these changes more precisely. Also, as people age, calcification changes in this gland can effectively influence these connections. However, this study can create a new perspective on the connections of the PG gland and its role. Further studies in this field may open new windows to investigate neurological diseases, such as Autism. Furthermore, we want to propose that meditation can cause activation of the PG body and increase resting-state functional connectivity in different parts of the brain. This includes the posterior cingulate cortex and the right middle temporal region.

5. Conclusion

Our study aimed to investigate the functional connections of the pineal gland (PG) with other brain regions and examine the structural correlations of the PG by mapping the tracts connected to it. While our findings contribute to the existing literature on the anatomy and function of the PG, we acknowledge several specific limitations that may affect the reliability and validity of our results.

Firstly, the use of a single b-value in diffusion tensor imaging (DTI) analysis may restrict our ability to fully capture the intricacies of white matter structure, potentially limiting the accuracy of the tract mapping associated with the PG. Secondly, our study lacked a directional approach in the functional connectivity analysis, which may hinder the assessment of the flow of information between the PG and other brain regions. Thirdly, we did not include comprehensive cognitive assessments that could link PG function and structure with specific cognitive abilities, leaving a gap in understanding its role in various cognitive processes. and its potential variability across individuals with different cognitive profiles. Furthermore, the study did not explicitly investigate gender differences, despite known hormonal variations that could influence PG connectivity.

Despite these limitations, our study suggests that the PG is connected to several brain regions involved in attention, memory, and emotion regulation. As demonstrated by functional connectivity analyses, meditation can cause activation of the PG body and increase resting-state functional connectivity in regions like the posterior cingulate cortex (PCC), suggesting a link between PG activation and default mode network (DMN) activity. However, these meditation-induced changes may vary across individuals with different levels of meditation experience. These connections may be essential for the PG's role in modulating cognitive processes and behavior. However, the strength and nature of these connections, and their influence on cognition and behavior, may vary significantly across different age groups, genders, and clinical populations. Specifically, the significant correlation between PG gland connections and age, as identified in our study, indicates that the observed connectivity patterns may not directly translate to younger or older populations due to developmental and calcification-related changes.

To build on the results of our study and address its limitations, we suggest the following future research directions:

1. Incorporating multi-shell DTI methods would provide a more comprehensive characterization of white matter microstructure, enabling a more accurate mapping of tracts connected to the PG.

2. Utilizing directional approaches, such as effective connectivity models, would allow researchers to investigate the flow of information between the PG and other brain regions, providing a more complete understanding of its functional role.

3. Including assessments of cognitive functions such as memory, executive function, and emotional regulation would facilitate the identification of associations between PG structure or function and cognitive abilities. By linking PG activity with performance on these assessments, future studies can deepen insights into how this gland modulates cognition and behavior.

4. Conducting longitudinal studies could help in understanding how PG connectivity and function evolve over time, especially in relation to aging or during different life stages, shedding light on its role in various developmental processes and potential adaptations.

5. Exploring the interplay between the PG and other hormonal systems, such as the hypothalamic-pituitary-adrenal (HPA) axis, could offer insights into how the PG influences not just cognitive functions but also emotional and physiological responses to stress. Understanding these interactions is crucial for understanding potential gender differences and variations in stress response across individuals. Additionally, investigating the role of the suprachiasmatic nucleus (SCN), as the main circadian pacemaker regulating melatonin secretion, could further elucidate the PG's hormonal influences.

6. Investigating the potential impact of neurodegenerative conditions on PG structural and functional connectivity could provide valuable information about its role in neurological disorders, enhancing our understanding of its significance in health and disease.

In conclusion, our study enhances the existing literature on the anatomy and function of the PG by highlighting its connections with different brain regions. However, we explicitly acknowledge the limitations of our study, which include the use of a single b-value in DTI analysis, the lack of a directional approach in functional connectivity analysis, and the absence of comprehensive cognitive assessments. By addressing these limitations and exploring new research avenues, such as longitudinal studies and investigations of hormonal interactions, future studies can further elucidate the PG's role in modulating cognitive processes and behaviors, ultimately contributing to a more comprehensive understanding of this enigmatic gland. Additionally, it is important to be cautious in interpreting DTI and fMRI results, as the relationship between structural connectivity and functional connectivity is complex, and one should avoid implying causation from correlational data.

References

1- Foroogh Razavi, Samira Raminfard, Hadis Kalantar Hormozi, Minoo Sisakhti, and Seyed Amir Hossein Batouli, "A probabilistic atlas of the pineal gland in the standard space." *Frontiers in neuroinformatics,* Vol. 15p. 554229, (2021).

2- Lisa A Ostrin, "Ocular and systemic melatonin and the influence of light exposure." *Clinical and experimental optometry,* Vol. 102 (No. 2), pp. 99-108, (2019).

3- Russel J Reiter, "The mammalian pineal gland: structure and function." *American Journal of Anatomy,* Vol. 162 (No. 4), pp. 287-313, (1981).

4- Morten Møller and Florian M Baeres, "The anatomy and innervation of the mammalian pineal gland." *Cell and tissue research,* Vol. 309pp. 139-50, (2002).

5- Ingo Nölte *et al.*, "Pineal volume and circadian melatonin profile in healthy volunteers: an interdisciplinary approach." *Journal of Magnetic Resonance Imaging: An Official Journal of the International Society for Magnetic Resonance in Medicine,* Vol. 30 (No. 3), pp. 499-505, (2009).

6- M Mila Macchi and Jeffrey N Bruce, "Human pineal physiology and functional significance of melatonin." *Frontiers in neuroendocrinology,* Vol. 25 (No. 3-4), pp. 177-95, (2004).

7- Inger Christine Munch, Morten Møller, Philip J Larsen, and Niels Vrang, "Light-induced c-Fos expression in suprachiasmatic nuclei neurons targeting the paraventricular nucleus of the hamster hypothalamus: phase dependence and immunochemical identification." *Journal of Comparative Neurology,* Vol. 442 (No. 1), pp. 48-62, (2002).

8- Tsutomu Takahashi *et al.*, "Reduced pineal gland volume across the stages of schizophrenia." *Schizophrenia Research,* Vol. 206pp. 163-70, (2019).

9- Minoo Sisakhti, Lida Shafaghi, and Seyed Amir Hossein Batouli, "The Volumetric Changes of the Pineal Gland with Age: An Atlas-based Structural Analysis."

Experimental Aging Research, Vol. 48 (No. 5), pp. 474-504, (2022).

10- Seyed Amir Hossein Batouli and Minoo Sisakhti, "Investigating a hypothesis on the mechanism of long-term memory storage." *NeuroQuantology,* Vol. 17 (No. 3), p. 60, (2019).

11- Martin Grosshans *et al.*, "The association of pineal gland volume and body mass in obese and normal weight individuals: A pilot study." *Psychiatria danubina,* Vol. 28 (No. 3), pp. 220-24, (2016).

12- V Aleandri, V Spina, and A Ciardo, "The role of the pineal body in the endocrine control of puberty." *Minerva Ginecologica,* Vol. 49 (No. 1-2), pp. 43-48, (1997).

13- D Larry Sparks and John C Hunsaker III, "The pineal gland in sudden infant death syndrome: preliminary observations." *Journal of pineal research,* Vol. 5 (No. 1), pp. 111-18, (1988).

14- Jan Malte Bumb *et al.*, "Associations of pineal volume, chronotype and symptom severity in adults with attention deficit hyperactivity disorder and healthy controls." *European Neuropsychopharmacology,* Vol. 26 (No. 7), pp. 1119-26, (2016).

15- Yaniv Assaf and Ofer Pasternak, "Diffusion tensor imaging (DTI)-based white matter mapping in brain research: a review." *Journal of molecular neuroscience,* Vol. 34pp. 51-61, (2008).

16- P Kochunov *et al.*, "Fractional anisotropy of water diffusion in cerebral white matter across the lifespan." *Neurobiology of aging,* Vol. 33 (No. 1), pp. 9-20, (2012).

17- Bennett A Landman, Jonathan AD Farrell, Craig K Jones, Seth A Smith, Jerry L Prince, and Susumu Mori, "Effects of diffusion weighting schemes on the reproducibility of DTI-derived fractional anisotropy, mean diffusivity, and principal eigenvector measurements at 1.5 T." *Neuroimage,* Vol. 36 (No. 4), pp. 1123-38, (2007).

18- Marco Catani and Michel Thiebaut De Schotten, "A diffusion tensor imaging tractography atlas for virtual in vivo dissections." *cortex,* Vol. 44 (No. 8), pp. 1105-32, (2008).

19- José M Soares, Paulo Marques, Victor Alves, and Nuno Sousa, "A hitchhiker's guide to diffusion tensor imaging." *Frontiers in neuroscience,* Vol. 7p. 31, (2013).

20- Ben Jeurissen, Alexander Leemans, Derek K Jones, Jacques-Donald Tournier, and Jan Sijbers, "Probabilistic fiber tracking using the residual bootstrap with constrained spherical deconvolution." *Human brain mapping,* Vol. 32 (No. 3), pp. 461-79, (2011).

21- Ardian Hana, Anisa Hana, Georges Dooms, Hans Boecher-Schwarz, and Frank Hertel, "Visualization of the medial forebrain bundle using diffusion tensor imaging." *Frontiers in Neuroanatomy,* Vol. 9p. 139, (2015).

22- Arash Kamali *et al.*, "Revealing the ventral amygdalofugal pathway of the human limbic system using high spatial resolution diffusion tensor tractography." *Brain Structure and Function,* Vol. 221pp. 3561-69, (2016).

23- Kat Christiansen *et al.*, "Topographic separation of fornical fibers associated with the anterior and posterior hippocampus in the human brain: An MRI-diffusion study." *Brain and behavior,* Vol. 7 (No. 1), p. e00604, (2017).

24- Gianvincenzo Sparacia, Giuseppe Parla, Giuseppe Mamone, Mariangela Caruso, Fabio Torregrossa, and Giovanni Grasso, "Resting-State Functional Magnetic Resonance Imaging for Surgical Neuro-Oncology Planning: Towards a Standardization in Clinical Settings." *Brain Sciences,* Vol. 11 (No. 12), p. 1613, (2021).

25- Xiaoli Wu *et al.*, "Circadian rhythm disorders and corresponding functional brain abnormalities in young female nurses: a preliminary study." *Frontiers in neurology,* Vol. 12p. 664610, (2021).

26- Chien-Hui Liou, Chang-Wei Hsieh, Chao-Hsien Hsieh, Jyh-Horng Chen, Chi-Hong Wang, and Si-Chen Lee, "Studies of Chinese original quiet sitting by using functional magnetic resonance imaging." in *2005 IEEE Engineering in Medicine and Biology 27th Annual Conference*, (2006): *IEEE*, pp. 5317-19.

27- Tali Gorfine, Yaniv Assaf, Yonatan Goshen-Gottstein, Yaara Yeshurun, and Nava Zisapel, "Sleep-anticipating effects of melatonin in the human brain." *Neuroimage,* Vol. 31 (No. 1), pp. 410-18, (2006).

28- Ahmed M Radwan *et al.*, "A comparison of diffusion MRI presurgical tractography techniques with intraoperative mapping-based validation." *medRxiv,* p. 2023.06. 13.23290806, (2023).

29- Andrey Zhylka, Alexander Leemans, Josien PW Pluim, and Alberto De Luca, "Anatomically informed multi-level fiber tractography for targeted virtual dissection." *Magnetic Resonance Materials in Physics, Biology and Medicine,* Vol. 36 (No. 1), pp. 79-93, (2023).

30- B Stieltjes, M Schlüter, HK Hahn, T Wilhelm, and M Essig, "Diffusions-Tensor-Bildgebung: Theorie, Sequenzoptimierung und Anwendungen bei Morbus Alzheimer." *Der Radiologe,* Vol. 43pp. 562-65, (2003).

31- Julie D Henry and John R Crawford, "The short-form version of the Depression Anxiety Stress Scales (DASS-21): Construct validity and normative data in a large non-clinical sample." *British journal of clinical psychology,* Vol. 44 (No. 2), pp. 227-39, (2005).

32- Seyed Amir Hossein Batouli and Minoo Sisakhti, "Some points to consider in a task-based fMRI study: A guideline for beginners." *Frontiers in Biomedical Technologies,* (2020).

33- Marco Catani, Derek K Jones, Rosario Donato, and Dominic H Ffytche, "Occipito-temporal connections in the human brain." *Brain,* Vol. 126 (No. 9), pp. 2093-107, (2003).

34- Marco Catani, Derek K Jones, and Dominic H Ffytche, "Perisylvian language networks of the human brain." *Annals of Neurology: Official Journal of the American Neurological Association and the Child Neurology Society,* Vol. 57 (No. 1), pp. 8-16, (2005).

35- Sang Seok Yeo, Jeong Pyo Seo, Yong Hyun Kwon, and Sung Ho Jang, "Precommissural fornix in the human brain: a diffusion tensor tractography study." *Yonsei Medical Journal,* Vol. 54 (No. 2), pp. 315-20, (2013).

36- Bram Stieltjes *et al.*, "Diffusion tensor imaging and axonal tracking in the human brainstem." *Neuroimage,* Vol. 14 (No. 3), pp. 723-35, (2001).

37- Sung Ho Jang and Jeong Pyo Seo, "The anatomical location of the corticobulbar tract at the corona radiata in the human brain: diffusion tensor tractography study." *Neuroscience Letters,* Vol. 590pp. 80-83, (2015).

38- Shawna Farquharson *et al.*, "White matter fiber tractography: why we need to move beyond DTI." *Journal of neurosurgery,* Vol. 118 (No. 6), pp. 1367-77, (2013).

39- Aurea Susana Blancas-Velazquez, Tenna Bering, Signe Bille, and Martin Fredensborg Rath, "Role and neural regulation of clock genes in the rat pineal gland: Clock modulates amplitude of rhythmic expression of Aanat encoding the melatonin-producing enzyme." *Journal of pineal research,* (2023).

40- Kristin Koller, Robert D Rafal, and Paul G Mullins, "Circadian circuits in humans: white matter microstructure predicts daytime sleepiness." *cortex,* Vol. 122pp. 97-107, (2020).

41- Catie Chang and Gary H Glover, "Effects of model-based physiological noise correction on default mode network anti-correlations and correlations." *Neuroimage,* Vol. 47 (No. 4), pp. 1448-59, (2009).

42- Chien-Hui Liou, Chang-Wei Hsieh, Chao-Hsien Hsieh, Si-Chen Lee, Jyh-Horng Chen, and Chi-Hong Wang, "Correlation between pineal activation and religious meditation observed by functional magnetic resonance imaging." *Nature Precedings,* pp. 1-1, (2007).

43- Zongpai Zhang *et al.*, "Longitudinal effects of meditation on brain resting-state functional connectivity." *Scientific reports,* Vol. 11 (No. 1), p. 11361, (2021).

44- Xiaoli Wu, Fan Bai, Yunlei Wang, and Lu Zhang, "Circadian rhythm disorders and corresponding functional brain abnormalities in young female nurses: a preliminary study." *Frontiers in neurology,* Vol. 12p. 664610, (2021).

45- Antoine R Adamantidis, Carolina Gutierrez Herrera, and Thomas C Gent, "Oscillating circuitries in the sleeping brain." *Nature Reviews Neuroscience,* Vol. 20 (No. 12), pp. 746-62, (2019).

46- Simone Cauzzo *et al.*, "Functional connectome of brainstem nuclei involved in autonomic, limbic, pain and sensory processing in living humans from 7 Tesla resting state fMRI." *Neuroimage,* Vol. 250p. 118925, (2022).

47- Elise R Facer-Childs, Brunno M Campos, Benita Middleton, Debra J Skene, and Andrew P Bagshaw, "Circadian phenotype impacts the brain's resting-state functional connectivity, attentional performance, and sleepiness." *Sleep,* Vol. 42 (No. 5), p. zsz033, (2019).

48- Martin A Koch, David G Norris, and Margret Hund-Georgiadis, "An investigation of functional and anatomical connectivity using magnetic resonance imaging." *Neuroimage,* Vol. 16 (No. 1), pp. 241-50, (2002).

49- Michael D Greicius, Ben Krasnow, Allan L Reiss, and Vinod Menon, "Functional connectivity in the resting brain: a network analysis of the default mode hypothesis." *Proceedings of the national academy of sciences,* Vol. 100 (No. 1), pp. 253-58, (2003).

50- Marcus E Raichle, Ann Mary MacLeod, Abraham Z Snyder, William J Powers, Debra A Gusnard, and Gordon L Shulman, "A default mode of brain function." *Proceedings of the national academy of sciences,* Vol. 98 (No. 2), pp. 676-82, (2001).

51- Michael D Greicius, Kaustubh Supekar, Vinod Menon, and Robert F Dougherty, "Resting-state functional connectivity reflects structural connectivity in the default mode network." *Cerebral cortex,* Vol. 19 (No. 1), pp. 72-78, (2009).

Table 3. The table provides the functional connectivity of different brain regions with the pineal gland; the beta value of the correlation, the t-value, and the FDR-corrected p-value of the correlations are also provided

Brain Regions	beta	T(282)	p-FDR
Vermis	0.27	4.14	0.001077
Superior Temporal Gyrus	0.26	3.91	0.002132
Subcallosal Cortex	0.26	3.85	0.002399
R Middle Temporal Gyrus	0.23	3.38	0.008025
Brain-Stem	0.19	2.89	0.025435
R Middle Frontal Gyrus	-0.18	-2.76	0.035763
R Frontal Pole	-0.18	-2.67	0.044642
L Fusifom	-0.18	-2.66	0.044798
L FrontoParietal cortex	-0.18	-2.64	0.04627
L Frontal Pole	-0.2	-3.07	0.018596
L Cuneus	-0.2	-3.01	0.021146
L Postcentral Gyrus	-0.2	-2.29	0.021146
R Intracalcarine Cortex	-0.2	-2.97	0.021146
L Supramarginal Gyrus	-0.2	-2.96	0.021146
L Supramarginal Gyrus	-0.21	-3.13	0.016097
R Accumbens	-0.22	-3.32	0.009323
R Cerebellum	-0.23	-3.51	0.00628
L Intracalcarine Cortex	-0.23	-3.49	0.00628
R Superior Parietal	-0.23	-3.45	0.006743
L Angular Gyrus	-0.24	-3.57	0.005899
L Lateral Occipital cortex	-0.25	-3.74	0.003431
L Superior Parietal	-0.28	-4.3	0.000803
R Cuneus	-0.28	-4.15	0.001077
Precuneous Cortex	-0.37	-5.55	0.000005